



**University of
Zurich**^{UZH}

**Zurich Open Repository and
Archive**

University of Zurich
University Library
Strickhofstrasse 39
CH-8057 Zurich
www.zora.uzh.ch

Year: 2008

The inhomogeneous background of H₂ dissociating radiation during cosmic reionization

Ahn, K ; Shapiro, P R ; Iliev, I T ; Mellema, G ; Pen, U L

DOI: <https://doi.org/10.1063/1.2905584>

Posted at the Zurich Open Repository and Archive, University of Zurich

ZORA URL: <https://doi.org/10.5167/uzh-17705>

Book Section

Accepted Version

Originally published at:

Ahn, K; Shapiro, P R; Iliev, I T; Mellema, G; Pen, U L (2008). The inhomogeneous background of H₂ dissociating radiation during cosmic reionization. In: O'Shea, B W; Heger, A. First stars III. Santa Fe, New Mexico, 15 - 20 July 2007. Melville NY: American Institut of Physics, 374-376.

DOI: <https://doi.org/10.1063/1.2905584>

The Inhomogeneous Background of H₂ Dissociating Radiation During Cosmic Reionization

Kyungjin Ahn^{*,†}, Paul R. Shapiro[†], Ilian T. Iliev^{**}, Garrelt Mellema[‡] and Ue-Li Pen[§]

^{*}*Department of Earth Science, Chosun University, Gwangju 501-759, Korea*

[†]*Department of Astronomy, 1 University Station, C1400, Austin TX 78712*

^{**}*Universitaet Zuerich, Institut fuer Theoretische Physik, Winterthurerstrasse 190 CH-8057 Zuerich, Switzerland*

[‡]*Department of Astronomy, Stockholm University SE-106 91 Stockholm, Sweden*

[§]*Canadian Institute for Theoretical Astrophysics, University of Toronto, 60 St. George St., Toronto, ON M5S 3H8, Canada*

Abstract. The first, self-consistent calculations of the cosmological H₂ dissociating UV background produced during the epoch of reionization (EOR) by the sources of reionization are presented. Large-scale radiative transfer simulations of reionization trace the impact of all the ionizing starlight on the IGM from all the sources in our simulation volume down to dwarf galaxies of mass $\sim 10^8 M_\odot$, identified by very high-resolution N-body simulations, including the self-regulating effect of IGM photoheating on dwarf galaxy formation. The UV continuum emitted below 13.6 eV by each source is then transferred through the same IGM, attenuated by atomic H Lyman series resonance lines, to predict the evolution of the inhomogeneous background in the Lyman-Werner band of H₂ between 11 and 13.6 eV.

Keywords: cosmology: theory – diffuse radiation – intergalactic medium – large-scale structure of universe – galaxies: formation

PACS: 98.65.Dx, 98.80.-k, 95.30.Jx

SUPPRESSION OF MINIHALO POP III STAR FORMATION BY H₂ DISSOCIATING UV BACKGROUND

Simulations suggest that first stars formed inside minihalos of mass $M \sim 10^6 M_\odot$ at $z \gtrsim 20$, when H₂ cooled the primordial, metal-free halo gas and gravitational collapse ensued. Formation of first stars inside minihalos, however, is suppressed when H₂ cooling is suppressed due to a strong H₂ Lyman-Werner(LW) band radiation field. This process occurs when the LW intensity J_{LW} exceeds the threshold LW intensity $(J_{LW})_{\text{threshold}}$, which is usually set by requiring that cooling time equals the dynamical time (e.g. Haiman, Rees & Loeb 1997).

It is important, therefore, to correctly calculate the rise of H₂ dissociating background in the Universe. Earlier estimates (e.g. Haiman, Abel & Rees 2000) found that sources of reionization made $J_{LW} > (J_{LW})_{\text{threshold}}$ long before reionization is complete, thus sterilizing minihalos before they could contribute significant reionization.

The LW background intensity would show spatial fluctuation due to the inhomogeneous distribution of reionization sources. However, previous calculations are based upon a homogeneous universe approximation. In these calculations, the sources and the IGM opacity were both uniformly distributed, in space with uniform emissivity given either by analytical approximation (e.g. Haiman, Abel & Rees 2000), or by sum over sources found in small-box simulations, too small to account for

large-scale clustering of sources or follow global reionization (e.g. Ricotti, Gnedin & Shull 2002; Yoshida et al. 2003).

Here we present the first self-consistent radiative transfer calculations of the inhomogeneous LW background produced by the same sources which reionized the universe in a large-scale radiative transfer simulation of reionization. We show that the fluctuation is significant enough to induce widely-different evolutionary history in the first star formation in different parts of the Universe.

A METHOD TO CALCULATE THE INHOMOGENEOUS LW BACKGROUND DURING EPOCH OF REIONIZATION

Calculating the inhomogeneous build-up of the LW background is computationally challenging. First, the mean free path for LW photons (~ 100 cMpc) is much larger than the mean free path for H ionizing photons. We need to account for sources distributed over large volume and look-back time. Second, LW band photons redshift and get attenuated by H atom Lyman series resonance lines as they travel through the expanding universe. This requires a multi-frequency radiative transfer calculation in a cosmological volume ($\gtrsim (100 \text{ cMpc})^3$), which is very expensive computationally.

We have developed a simple, yet accurate method

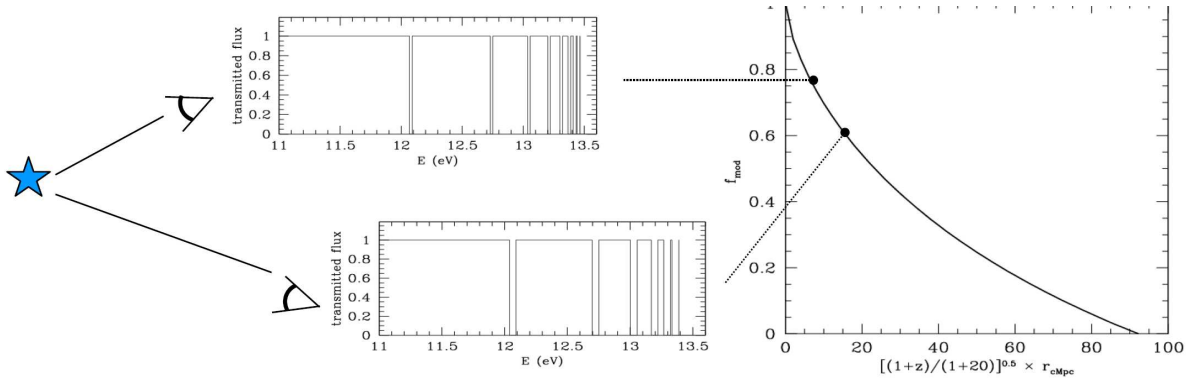


FIGURE 1. “picket-fence” modulation. A source observed at different places suffers different amounts of attenuation, dilution, and redshift. As continuum (flat-spectrum assumed) photons redshift, all the photons which have redshifted to H atom resonance lines are turned into low-energy photons. This leaves gaps in observed spectrum, which depend on the distance to the source. The modulation factor (right panel) is the effective transmission rate, which drops as the distance increases, until source is completely attenuated at $r_{\text{cMpc}} = 92[(1+z)/21]^{-0.5}$. With this modulation factor, we are able to compute LW intensity without costly multi-frequency calculation.

to calculate the radiative transfer of LW band photons, which alleviates the need for a multi-frequency calculation. This is achieved by using a pre-computed modulation factor, expressed in terms of the comoving distance between a source and an observer, that accounts for the attenuation of LW band photons from a single source. We call this a “picket-fence” modulation factor f_{mod} , after the shape of the LW intensity J_{ν} which is composed of both attenuated and unattenuated parts (Fig. 1). The picket-fence modulation factor is computed by averaging a normalized J_{ν} (at $r_{\text{cMpc}}(z_s, z_{\text{obs}})$) over frequency in the range of [11.5 – 13.6] eV.

At a given point in space, one then looks back in time to search for sources located inside the LW band horizon (~ 100 cMpc). For each source found this way, a “bare” flux is obtained from its luminosity L_{ν} and the luminosity distance, which corresponds to a flux in an optically thin limit. This is then multiplied by f_{mod} to account for the attenuation by H atom Lyman series resonance lines. Since f_{mod} is a function of the comoving distance only, an expensive multi-frequency calculation is not required. When looking back in time for contributing sources, we draw past light-cones in order to account for the retarded time effect due to finite light-crossing time (Fig. 2). Sources are distributed in a discrete sense in time, following our reionization simulations results (e.g. Iliev et al. 2007).

INHOMOGENEOUS LW BACKGROUND

In order to calculate inhomogeneous LW background, we use “self-regulated” reionization simulation results by Iliev et al. (2007). Their radiative transfer calculation is based upon an N-body simulation (1624^3 particles

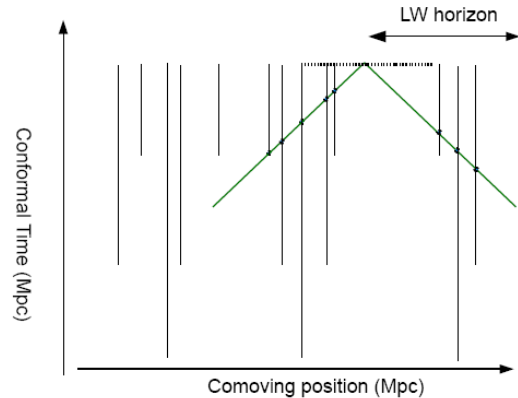


FIGURE 2. Conformal spacetime diagram, to be used to calculate source contribution from cosmological distances. Each source contributes LW flux of $f_{\text{mod}}L/D_L^2$, where L is luminosity, D_L is the luminosity distance to the source, and f_{mod} is the picketfence modulation factor which accounts for IGM opacity. This scheme naturally accounts for the finite light-crossing time of radiation.

and 3248^3 cells) result which provides the source catalogue for H-ionizing radiative transfer calculation. This resolves halos of mass $M/M_{\odot} \gtrsim 10^8$, thus accounting for all atomic cooling halos in the $(50\text{cMpc})^3$ volume. Source formation is self-regulated: formation of sources inside small-mass halos ($10^8 < M/M_{\odot} < 10^9$) is suppressed if H II regions overtake their formation sites. We then use a coarse-grained mesh (203^3 cells) to calculate the fluctuating LW radiation field. To account for the large LW band horizon, we distribute sources periodically around the box where the LW background is calculated.

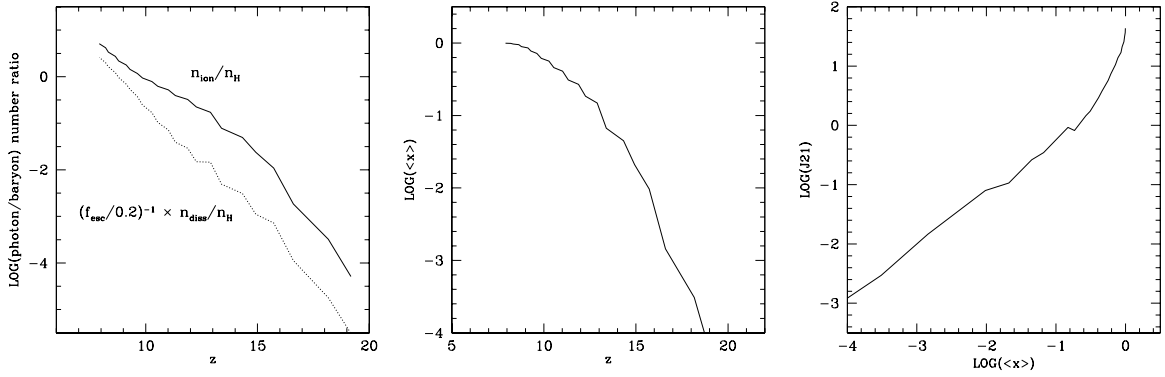


FIGURE 3. Global history of cosmic reionization and LW intensity evolution. (Left): The accumulated number of ionizing photons per baryon vs. the number of dissociating photons per baryon. (Middle): Global evolution of ionization fraction $\langle x \rangle$. (Right): Global evolution of LW intensity J_{21} . Note that if reionization source properties change, especially in ionizing photon escape fraction (f_{esc}) and ratio of dissociating/ionizing photons, J_{21} may differ even at the same global ionized fraction.

We chose an illustrative case, WMAP3 f2000_250S, among the reionization simulation results by Iliev et al. (2007). For small mass halos ($10^8 < M/M_\odot < 10^9$), Pop III high efficiency emitters with top-heavy IMF are assumed, with $f_\gamma = f_* \cdot f_{\text{esc}} \cdot N_i = 2000$, and with $N_i/N_{\text{diss}} \simeq 15$, where f_* is the star formation efficiency, f_{esc} is the ionizing photon escape fraction, N_i is the number of ionizing photons emitted per baryon, and N_{diss} is the number of H_2 dissociating photons emitted per baryon. Formation of sources inside large-mass halos ($M > 10^9 M_\odot$) are not suppressed even inside H II regions. Pop II low efficiency emitters with Salpeter IMF are assumed, with $f_\gamma = f_* \cdot f_{\text{esc}} \cdot N_i = 250$, and with $N_i/N_{\text{diss}} \simeq 1$.

Fig. 3 summarizes our result on the global ionized fraction $\langle x \rangle$ and the mean LW intensity $\langle J_{21} \rangle$. We find that $\langle J_{21} \rangle$ is dominated by small mass halo contribution initially, while at later epoch by large-mass halo contribution in this case. By the time large mass halos become important, most of small mass halos are already inside H II regions and get sterilized. If reionization source properties were different from our illustrative case, however, especially in f_{esc} and N_i/N_{diss} , the same $\langle x \rangle$ would not mean the same J_{21} , in general.

A significant inhomogeneity in the LW background is apparent, with fluctuation scale of a few ~ 10 cMpc (Fig. 4). This is due to a highly-clustered source distribution, which shows a fluctuation scale of a similar kind. This will induce an inhomogeneous LW feedback, hence inhomogeneous minihalo star formation rate. The most pristine environment will be found where the most active minihalo star formation activity occurs. Those sites would exist where the LW intensity becomes minimum, as shown in Fig. 4. These first-star forming regions during the epoch of reionization might be detected by upcoming telescopes such as the James Webb Space Telescope (JWST).

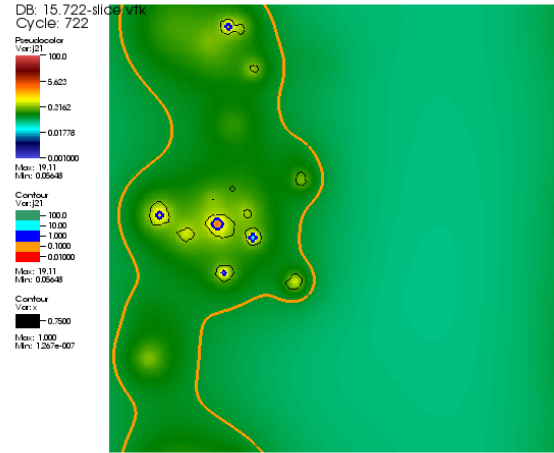


FIGURE 4. Patchy reionization and patchy H_2 dissociating background in $(50 \text{ cMpc})^3$ box at $z = 15.7$. Contours of thick colored lines represent different J_{21} contours (orange – $J_{21} = 0.1$; blue – $J_{21} = 1$), and the black contours represent the ionization fronts. Minihalos are subject to spatially-varying LW feedback effect, thus yielding spatially-varying minihalo star formation rate. JWST may able to detect clustered minihalo population at $z \sim 15$ in regions of least LW feedback.

REFERENCES

1. Haiman, Z., Abel, T., & Rees, M. 2000, ApJ, 534, 11
2. Haiman, Z., Rees, M. J., & Loeb, A. 1997, ApJ, 476, 458
3. Iliev, I. T., Mellema, G., Shapiro, P. R., & Pen, U. L. 2007, MNRAS, 376, 534
4. Ricotti, M., Gnedin, N. Y., & Shull, J. M. 2002, ApJ, 575, 33
5. Yoshida, N., Abel, T., Hernquist, L., & Sugiyama, N. 2003, ApJ, 592, 645